Atomic Force Microscopy to Study Intermolecular Forces and Bonds Associated with Bacteria

Steven K. Lower

(2011)

Advances in Experimental Medicine and Biology **715**: 285-299.

DOI 10.1007/978-94-007-0940-9_18

Chapter 18
Atomic Force Microscopy to Study Intermolecular Forces and Bonds Associated with Bacteria

Steven K. Lower

Abstract Atomic force microscopy (AFM) operates on a very different principle than other forms of microscopy, such as optical microscopy or electron microscopy. The key component of an AFM is a cantilever that bends in response to forces that it experiences as it touches another surface. Forces as small as a few picoNewtons can be detected and probed with AFM. AFM has become very useful in biological sciences because it can be used on living cells that are immersed in water. AFM is particularly useful when the cantilever is modified with chemical groups (e.g. amine or carboxylic groups), small beads (e.g. glass or latex), or even a bacterium. This chapter describes how AFM can be used to measure forces and bonds between a bacterium and another surface. This paper also provides an example of the use of AFM on *Staphylococcus aureus*, a Gram-positive bacterium that is often associated with biofilms in humans.

18.1 Introduction to AFM

In most microbiology laboratories, students are taught how to culture bacteria in enclosed vessels that contain nutrient broth. The growth cycle of a bacteria population is determined by measuring the optical density of cell suspensions. However, most bacteria do not naturally live as suspended entities within a solution. In nature, most bacteria live attached to or in contact with a solid surface (Parsek and Fuqua, 2004; Watnick and Kolter, 2000; Whitman et al., 1998). The planktonic mode of life is simply a means to move from one surface to another.

What forces allow a bacterium to make contact with an inorganic surface? How does a bacterium form a bond with a protein-coated material? It wasn't until very recently that we were able to directly probe the interface between a mineral or

S.K. Lower (✉)
Ohio State University, Columbus, OH 43210, USA
e-mail: lower.9@osu.edu

D. Linke, A. Goldman (eds.), *Bacterial Adhesion*, Advances in Experimental Medicine and Biology 715, DOI 10.1007/978-94-007-0940-9_18,

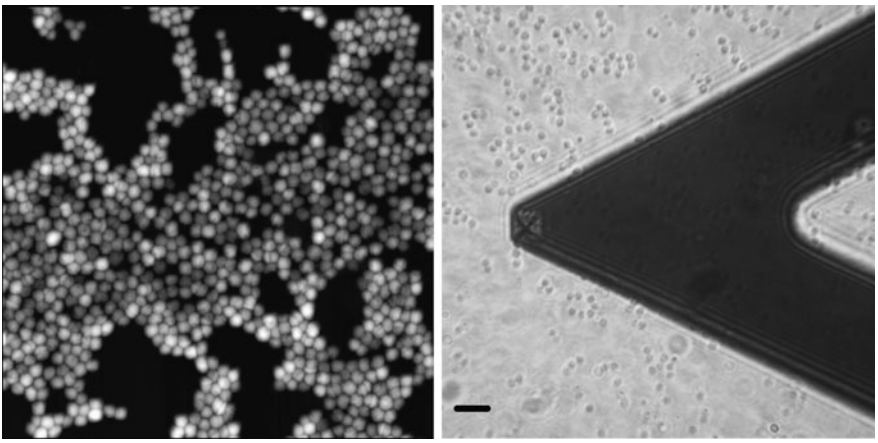

Fig. 18.1 (*Left*) Image of living *Staphylococcus aureus* on a glass slide immersed in a saline buffer. This image was collected with an AFM. The image size is 25 μm × 25 μm. (*Right*) Optical micrograph that shows the positions of the AFM cantilever and tip (square pyramid near end of cantilever) as well as cocci-shaped *S. aureus* cells on the glass slide. The bacteria are blurred because the plane of focus is on the AFM tip. Scale bar is approximately 10 μm

material and a living bacterium. The invention of the atomic force microscope (AFM) (Binnig et al., 1986) opened the door to investigations into the fundamental forces and bonds that control how a bacterium interacts with a solid surface.

Figure 18.1 shows the Gram-positive bacteria *Staphylococcus aureus* on a silica surface, that is, a glass slide. This image was collected by scanning a relatively sharp AFM tip over the *S. aureus* cells (see right image in Fig. 18.1). Images like this AFM micrograph provide a visual depiction of a bacterium in contact with another surface. However, the actual interface is hidden from view. One would need to probe under the bacterium to reveal the true region of interest.

Intermolecular forces, such as van der Waals, electrostatic, solvation, and steric interactions (Leckband and Israelachvili, 2001), control how a bacterium's cell wall physically interacts with another surface. The small magnitude of these forces and the small length scale over which they operate make it a challenge to probe these forces. AFM has the force- and space-sensitivity to accomplish this task. The first papers describing the use of AFM to study adhesion forces of bacteria began to appear in the literature about a decade ago (Camesano and Logan, 2000; Lower et al., 1999, 2000; Razatos et al., 1998). Since then, AFM has been used countless times to study the fundamental forces that direct adhesion and biofilm formation.

This chapter provides readers with a brief overview of AFM. For a more extensive review of AFM the reader is referred to the following publications: (Cappella and Dietler, 1999; Kendall and Lower, 2004; Yongsunthon and Lower, 2006). This chapter also provides examples to illustrate how AFM can be used to study (i) forces as a bacterium approaches a surface, and (ii) bonds that may rupture as a bacterium is pulled away from the surface. These examples will draw primarily upon my knowledge and experience with *S. aureus*.

18.2 The Main Components of AFM

AFM is a scanning probe microscopy instrument that consists of a force-sensing cantilever, a piezoelectric scanner, and a photodiode detector (Fig. 18.2). The cantilever bends upwards due to repulsive forces, or downwards due to attractive forces, between a sample (e.g. a bacterium) and a small tip that is an integrated part of the end of the cantilever. The deflection of the cantilever is monitored by reflecting a laser off the top of the free-end of the cantilever and into the photodetector.

The cantilever behaves like a spring such that the force (F in Newtons) acting on the cantilever tip is given by Hooke's Law $F = -(K_{sp})(x)$, where K_{sp} is the cantilever spring constant (N m^{-1}) and x is the deflection of the free-end of the lever (in m). The piezoelectric scanner moves the fixed-end of the cantilever towards and away from the sample (see Fig. 18.2), or in some systems the sample moves towards or away from the cantilever. In essence, the piezoelectric scanner allows one to precisely control the formation and subsequent destruction of a contact event between two surfaces. Simultaneously, the optical lever detection system of the AFM allows the quantitative measure of forces between the two surfaces.

This chapter will focus primarily on the one-dimension "force curves" that are generated as a cantilever tip is brought into contact with a bacterium and then pulled away from the bacterium. It is important to note that AFM can also be used to create a three-dimensional topographic image like the one shown in Fig. 18.1. This

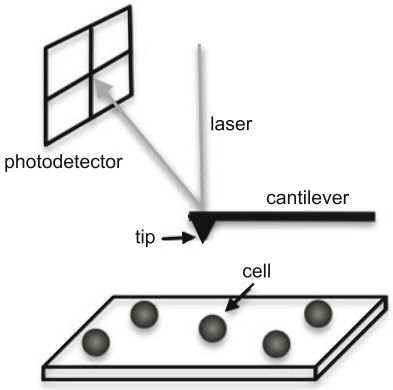

Fig. 18.2 Schematic diagram showing the key components of an AFM. A piezoelectric scanner (not shown) moves the "fixed end" of the cantilever relative to the sample (cell or substrate). Forces between the sample and tip cause the "free end" of the cantilever to deflect or bend. The behaviour of the cantilever is monitored by tracking a laser beam reflected off the top side of the cantilever and onto a photodetector. One can use this setup to measure forces as the tip approaches, makes contact with, and is subsequently retracted from the sample. A topographic image of the sample can also be collected by laterally scanning the tip across the sample while measuring the deflection of the cantilever

is accomplished by monitoring the vertical deflection of the cantilever as the tip is scanned laterally across the sample.

18.2.1 Modification of AFM Cantilever and Tip for Biological Experiments

Commercially available force-transducing cantilevers may be V-shaped silicon nitride levers or single beam silicon levers (Albrecht et al., 1990; Tortonese, 1997). However, these materials may not be the most interesting substrates for microbiological investigations. Therefore, the cantilever (or tip) is often modified prior to use. For example, the tip may be functionalised with various chemical groups (Noy et al., 1997). Small (2–10 μm radius) beads may be glued to the end of an AFM cantilever (Ducker et al., 1991, 1992). Living cells can even be linked to the end of an AFM cantilever (Lower et al., 2000, 2001b).

Figure 18.3 shows a glass bead, approximately 10 μm in diameter, on the end of the AFM cantilever. The tip is still visible in this image, although its size (~4 μm) means that a sample will interact with the bead rather than the tip. Figure 18.3 also shows a bacteria-coated bead on the end of an AFM cantilever. These cells on the end of the cantilever are living (Lower et al., 2000). A single bacterium can also be attached to an AFM tip (Jericho et al., 2004; Lower et al., 2001b).

It is important to note that a cantilever's nominal spring constant (N m^{-1}), as quoted by the manufacturer, can vary significantly from the actual value (Senden and Ducker, 1994). Therefore, one should always calibrate the spring constant of a cantilever. There are a number of methods including the Cleveland method (Cleveland et al., 1993), the hydrodynamic drag method (Craig and Neto, 2001), and the resonant frequency method (Hutter and Bechhoefer, 1993).

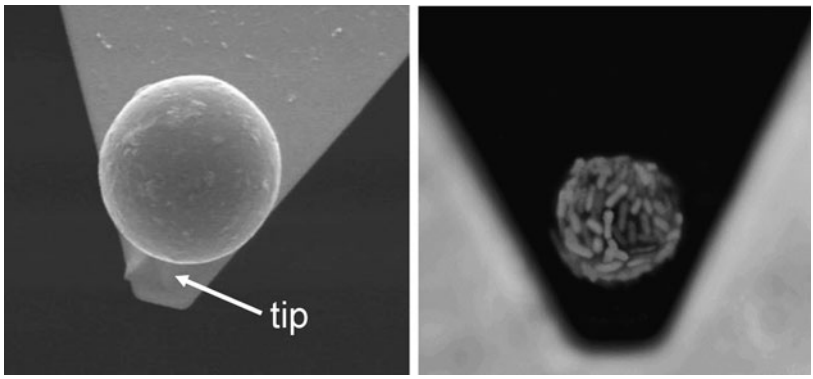

Fig. 18.3 (*Left*) Scanning electron microscopy image of a glass bead that is attached to the free end of the cantilever. (*Right*) Optical micrograph of a bacteria-coated bead on the end of the cantilever. The cells are expressing an intracellular green fluorescent protein so that they can be visualised on the cantilever

18.2.2 Collection and Analysis of Force Data

Each force curve consists of two parts: approach of the tip toward the sample and the subsequent retraction of the tip from the sample. The rate of the approach-retraction cycle may be controlled by the operator. A typical approach-retraction curve takes about 1 s.

In raw form, AFM force data are measured as (i) the output voltage from a photodiode detector in response to the deflection of the cantilever deflection, and (ii) the displacement (or movement) of the cantilever relative to the sample. To convert the raw measurements into meaningful physical quantities, the photodiode output voltage must be converted to force values and the displacement must be converted to distance or separation between the tip and sample.

18.2.2.1 Converting Photodetector Voltage into Force Values

The photodiode output signal, which is related to the position of the reflected laser spot (see Fig. 18.2), is measured in volts. These voltages correspond to the upwards or downwards movement of the free end of the cantilever in response to repulsive or attractive forces between the tip and sample. Detector voltage measurements must be converted into force values using the spring constant of the cantilever (N m^{-1}; see above) and a "volts to nm" conversion factor called the optical lever sensitivity (in nm V^{-1}).

The optical lever sensitivity allows the signal from the photodiode detector (in volts) to be converted into deflection (in nm) values for the cantilever. When the cantilever is pressed into contact with a hard surface, each unit of piezo movement ideally corresponds to an equivalent deflection of the cantilever. The inverse slope of the region of contact (also referred to as the region of constant compliance) is the optical lever sensitivity (Fig. 18.4). For the data shown in Fig. 18.4, the optical lever sensitivity is ~120 nm V^{-1}. Each voltage value is multiplied by the optical lever sensitivity to determine the upwards or downwards deflection of the cantilever in response to repulsive or attractive forces, respectively.

One important point to consider is that this conversion is accurate only if the cantilever itself is the most compliant or flexible component of the system. This includes not only the cantilever but also the sample and any cells or biological polymers that may be attached to the cantilever. This criterion may not be met for many soft materials such as biological cells. Therefore, it is best to calibrate the optical lever sensitivity on bare glass prior to measuring forces on bacteria that are deposited on the same piece of bare glass.

Once the photodiode signal (V) is converted into the deflection of the cantilever (m), the spring constant (N m^{-1}) is used to convert the deflection values into force data (N). The region of no contact is defined as zero force (see Fig. 18.4). Any value above this line (i.e. positive) indicates repulsion whereas any value below this line (i.e. negative) indicates attractive forces between the tip and sample.

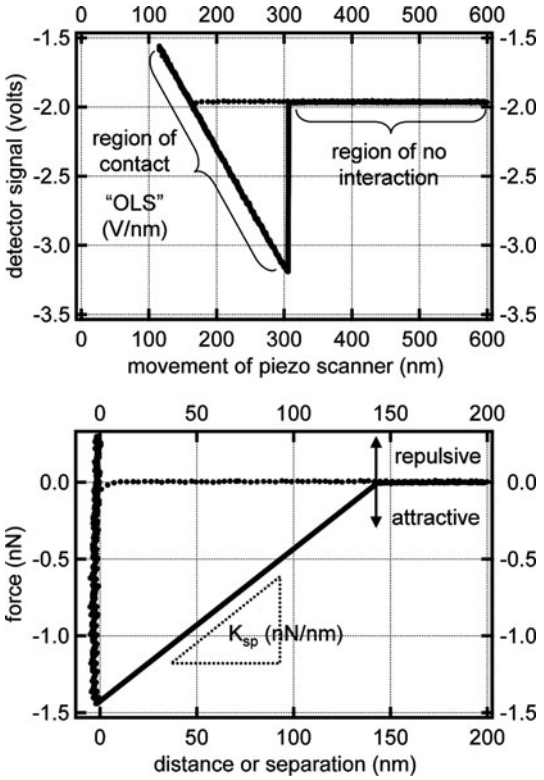

Fig. 18.4 (*Top*) The approach (*dotted*) and retraction (*solid*) curves for an AFM tip on a hard substrate. The y-axis shows the raw voltage output of the photodetector in response to the deflection of the free-end of the cantilever. The x-axis shows the vertical movement of the piezoelectric scanner, which translates the fixed-end of the cantilever. In the region of contact, each unit of piezo movement results in equivalent cantilever deflection (e.g. the cantilever deflects 1 nm if the piezo moves 1 nm). The inverse slope in this region yields the optical lever sensitivity, ~120 nm V^{-1}, which is a measure of how the photodetector responds to the flexure of the cantilever. (*Bottom*) The photodetector output (*top plot*) was converted to cantilever deflection (in nm) which in turn was converted to force, assuming a spring constant of 0.01 nN/nm. The piezo movement was corrected to account for deflection of the cantilever and yields the separation between tip and sample. By convention, repulsive forces are positive and attractive forces negative. The "jump-from" or "jump-to" contact features result from the mechanical instability of the cantilever relative to the forces it is probing. Jump-from contact features can be seen in retraction curves when the cantilever spring constant exceeds the actual force gradient at the tip-glass interface (K_{sp} label on *bottom figure*). Jump-to contact features may be present in approach data when the actual force gradient exceeds the spring constant of the cantilever (see distance from 0 to 10 nm in approach curve in the *bottom figure*)

18.2.2.2 Converting Piezoelectric Scanner Movement into Separation values

The movement of the piezoelectric scanner must be corrected by the deflection of the free end of the cantilever to obtain an absolute separation distance between a sample (e.g. a cell attached to a substrate) and the tip on the cantilever. The

separation between the tip and sample can be determined once the photodiode signal is converted into deflection values for the cantilever. Absolute separation is determined by correcting the movement of the piezoelectric scanner by the cantilever deflection. For example, if the piezoelectric scanner moves the cantilever 10 nm towards the sample, but the free end of the cantilever deflects upwards by 2 nm, the actual separation has changed by only 8 nm (Fig. 18.4).

The origin of the separation axis (i.e. distance of zero) is defined by using "jump-to-contact" and "jump-from-contact" events for approach and retraction curves, respectively (see Fig. 18.4). In instances where only repulsive forces are measured (i.e. no jump to/from contact) it is more difficult to define a separation distance of zero. This is typically accomplished by defining the initial point on the region of contact as the origin of the separation axis.

18.3 Examples of AFM Force Measurements on Living Bacteria

In the late 1990s, a few groups of researchers began to use AFM to study forces associated with bacterial adhesion (Camesano and Logan, 2000; Lower et al., 1999, 2000; Razatos et al., 1998). Since then there have been countless publications in which AFM has been used to probe forces and bonds associated with bacteria. Over the years, a number of researchers have led this effort, including Terrance Beveridge, Terri Camesano, Yves Dufrene, and the current author. Below I will provide two examples to illustrate how AFM can be used to gain a unique perspective of the forces, bonds, and macromolecules that operate at the interface between a bacterium and another surface.

18.3.1 Intermolecular Forces as Staphylococcus aureus Comes into Contact with Silica (SiO_2)

Quartz (SiO_2), or its amorphous form silica, is probably the most common surface that bacteria encounter in nature. This is mainly due to the fact that the two elements silicon and oxygen make up 74 wt% (95 vol%) of the Earth's crust (Klein and Hurlbut, 1985). On an atomic scale, the Earth's crust consists of a packing of oxygen atoms with interstitial metal ion, mainly Si. Quartz and silica are also found within humans in the form of implanted medical devices, like catheters for example. Bacteria are known to form infectious biofilms on such surfaces. Finally, silica glass slides are the substrate of choice for viewing bacteria with an optical microscope.

AFM can be used to measure the attractive or repulsive intermolecular forces that a bacterium experiences as it approaches a surface of quartz or silica. The following discussion will show force-distance curves that were collected between a glass bead attached to the end of a cantilever (Fig. 18.3, left panel), and living cells of *S. aureus*, which were sitting on a glass slide (Fig. 18.1, right panel). The observed force-distance relationship will be compared to theoretical models of two important

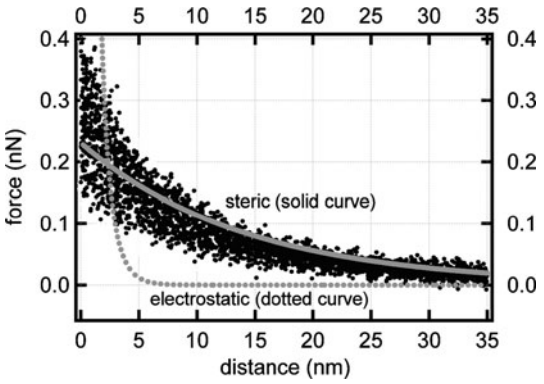

Fig. 18.5 Intermolecular forces (*dots*) measured as a 10 μm silica (SiO_2) bead approaches a *S. aureus* bacterium in 0.1 M NaCl solution at about pH 7. The electrostatic force was calculated using Eq. (1) with surface potentials of –35 and –6 mV for the silica and bacterium, respectively. The steric force was calculated using Eq. (2) with values of 90 nm and 3.4×10^{14} molecules per m^2 for the polymer thickness and density, respectively

intermolecular forces: the electrostatic force and the steric force. By comparing the measured and theoretical forces, one can determine which force type controls the initial adhesion of *S. aureus* to SiO_2 surfaces in an aqueous solution.

Figure 18.5 shows forces detected as a glass bead is brought into contact with a single cell or binary fission pair of *S. aureus*. Shown are 10–15 approach curves chosen at random from a total of ~500 curves collected for three different glass beads and three different cultures of the same strain of *S. aureus*. This figure reveals that the bead's surface must approach to within 30 nm of the bacterium before a measurable force is detected. As the distance between the cell and glass decreases, the bacterium experiences a repulsive force (positive sign) that appears to increase exponentially until the cell and glass make contact (i.e. a distance of zero).

Theoretical force-distance expressions can be used to interpret the observed force data. As mentioned in the Introduction, there are a few fundamental forces that may exist between surfaces in aqueous solution. The electrostatic force is one of these force types. A common mathematical expression for the electrostatic force is given as (Elimelech et al., 1995):

$$F(D) = \frac{2\,\pi\, r_1\, r_2\, \varepsilon\, \varepsilon_0\, \kappa}{r_1 + r_2} \left(\frac{k_B\, T}{z\, e_c} \right)^2 \frac{\phi_1^2 + \phi_2^2 + \left(2e^{D\kappa}\phi_1\phi_2\right)}{\left(e^{D\kappa} - 1\right)\left(e^{D\kappa} + 1\right)} \tag{1}$$

where F = force (in Newtons); D = distance between the two surfaces of interest (m); r = radius of the cell or bead (m), ε is the dielectric constant of water (78.54 at 298 K), ε_0 is the permittivity of free space (8.854×10^{-12} C^2 $J^{-1}m^{-1}$), k_B is Boltzmann's constant (1.381×10^{-23} J K^{-1}), T is temperature (298 K), z is the valence of electrolyte ions (1 for NaCl), and ec is the charge of an electron (1.602×10^{-19} C). The inverse Debye length (κ, in m^{-1}) describes the thickness of

the electrostatic double layer of counter-ions that surrounds charged particles (glass bead or bacterium) in solution. For monovalent electrolytes (e.g. NaCl) at 298 K, the Debye length (κ^{-1}, in nm) is given by $0.304/(c)^{-1/2}$, where c is the concentration of the electrolyte (mol L^{-1}). The final parameter is the surface potential (ϕ) described as [(zeψ)/(kT)], where ψ is the surface potential of the cell or glass bead (in V) and all other parameters are as described above.

For an aqueous solution at around pH 7 and ionic strength ~0.1 M, the surface potentials of a glass bead and *S. aureus* are, respectively, –35 mV (Ducker et al., 1992) and –6 mV (Prince and Dickinson, 2003). By using these values in Eq. (1), one may calculate the theoretical electrostatic force between an *S. aureus* bacterium and a glass bead. This theoretical force-distance relationship is shown in Fig. 18.5.

The electrostatic force is expected to be repulsive and short range (<5 nm) in a 0.1 M saline solution. While the observed interaction is repulsive, the measured forces are clearly longer range than expected based solely on electrostatic interactions. Therefore, another intermolecular force must also be involved in how this particular bacterium interacts with the surface of glass.

Staphylococcus cells, like all bacteria, have a surface that is studded with biological polymers. One of the most common biopolymers on *S. aureus* is β-1,6-linked glucosaminoglycan, also know as the polysaccharide intercellular adhesin (PIA) (Heilmann et al., 1996; Ziebuhr et al., 1997). Polymers such as these cause steric repulsion when they are confined to a narrow space (Israelachvili, 1992; Israelachvili and McGuiggan, 1988; Taylor and Lower, 2008). This repulsion is driven by a decrease in entropy that occurs when a polymer is no longer free to move at random. Polymers that are free to move and rotate in random orientations within a solution are in a higher state of disorder relative to the same polymer that has been confined to a smaller volume of space. This is precisely what occurs when a polymer on a bacterium is confined to a narrowing interface created by an approaching surface (e.g. a glass bead).

Like the electrostatic force (see Eq. (1)), the steric force (F) has been described as a function of the distance (D) between two surfaces. This expression, known as the modified Alexander-de Gennes equation, is given by (Butt et al., 1999; Taylor and Lower, 2008):

$$F(D) = 50\, r\, \mathrm{k_B}\, T\, L_0\, \Gamma^{3/2} e^{-2\pi D/L_0} \tag{2}$$

where r = radius of the cell (m), k_B is Boltzmann's constant (1.381 × 10–23 J K–1), T is temperature (298 K), L_0 is the equilibrium thickness of a polymer (in m) on the cell surface, Γ is the surface density of that same polymer on the cell surface (in m–2).

One can determine the theoretical steric force between *S. aureus* and glass by using the thickness and surface density of PIA. *Staphylococcus* have PIA molecules composed of at least 130 sugar residues (Mack et al., 1996), which corresponds to a value for L_0 of ~90 nm assuming 0.7 nm per glucose residue (Yongsunthon and Lower, 2006). While not measured directly, the surface density (Γ) of PIA on a staphylococci cell can be estimated from previous studies (Mack et al.,

1996; Madigan et al., 2003). Using these references, there are about 4300 PIA polysaccharides per bacterium. For a 2 μm bacterium (i.e. proxy for a fission pair of *Staphylococci* cells) this is equivalent to approximately 3.4×10^{14} PIA per m^2. Using these values for L_0 and Γ in Eq. (2) results in a theoretical expression of the steric force between a *Staphylococcus* cell and a glass bead (see Fig. 18.5).

Comparing the measured forces to the theoretical models reveals that the steric force and to a lesser extent the electrostatic force dominate the interactions between *S. aureus* and a glass surface in saline solution. The glass substrate must be within 30 nm of the bacterium surface before the forces between the two are measurable (above noise). Steric forces then cause the bacterium to be repelled until the cell is within ~5 nm of the glass. At this close distance, repulsive, electrostatic forces begin to impact the final approach.

18.3.2 Bonds that Form Between Staphylococcus aureus and a Silica Surface That Is Coated with a Protein Layer

The above example focuses only on the forces that occur as a cell approaches another surface. However, adhesion may occur and bonds may form once a cell comes into contact with another surface. AFM can be used to probe the force required to rupture a bond that forms between a biomolecule on a bacterium and a reactive site on a material surface. AFM can also be used the probe the biomechanical properties of cell wall macromolecules.

The following discussion will show force-distance curves that were collected as a protein coated probe was pulled from contact with living cells of *S. aureus*. For these measurements, the AFM tip was coated with fibronectin (Fn), a human protein that commonly coats implanted medical devices. The measured force-distance curves will be compared to a worm-like chain model, which predicts the force-distance trajectory for a protein that is mechanically perturbed into an unfolded conformation. By comparing the measured and theoretical forces, one can identify an adhesin and understand the intrinsic biomechanical properties of that adhesin.

Figure 18.6 shows the force-extension curves for Fn on a glass slide versus Fn in contact with a strain of *S. aureus* that overexpresses fibronectin-binding protein (FnBP) on its cell wall. Many of these curves exhibit a distinct, non-linear, sawtooth-shaped, force-distance relationship. For example, the Fn molecules (X-symbols in Fig. 18.6) unravel to approximately 200 nm where they rupture at a force of ~0.4 nN. This non-linear, sawtooth-shaped feature becomes more pronounced for Fn that has formed a bond with putative FnBPs on *S. aureus*.

Such signatures have been attributed to specific binding events mediated by proteins (Carrion-Vazquez et al., 1999; Lower et al., 2001a, 2005; Mueller et al., 1999; Müller et al., 1999; Oberdorfer et al., 2000; Oberhauser et al., 1999; Rief et al., 1997). The shape profile of the binding event can be explained by the unfolding mechanics of the bound protein. The worm-like chain (WLC) model approximates the biomechanical force-extension relationship of folded-polymers (e.g. proteins)

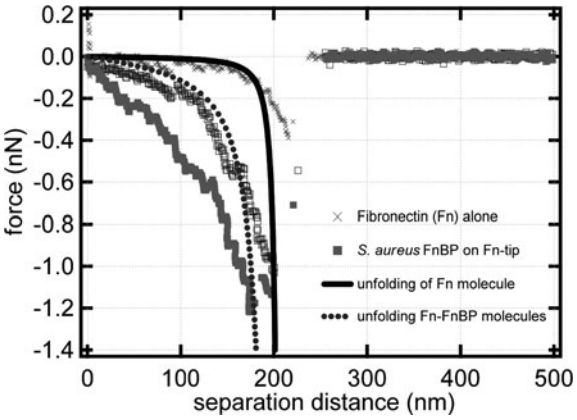

Fig. 18.6 Forces measured as a protein, which forms a bridging bond between two surfaces, is stretched or unfolded in a buffer solution. These retraction curves begin at the origin and proceed to the right on the distance axis. The "x" symbols correspond to a fibronectin (Fn) coated tip that is being pulled away from a glass slide. The *square symbols* correspond to an Fn-tip that has bonded to fibronectin-binding proteins (FnBP) on *S. aureus*. Equation (3) was used to calculate the theoretical force-extension relationship for a Fn molecule (*solid curve*) versus an Fn molecule that has formed parallel bonds with FnBP on the cell wall of a bacterium. For this calculation the contour length was 210 nm and the persistence length was 0.4 nm (*solid curve*) or 0.04 nm (*dotted curve*)

that are mechanically extended (or unfolded) into their linear form (Flory, 1989). The WLC equation is given as:

$$F(D) = [k_B T/p] \times [0.25\,(1 - D/L)^{-2} + D/L - 0.25], \tag{3}$$

where F (in Newtons) is the entropic restoring force generated when a protein is mechanically unfolded to distance D (in meters), k_B is Boltzmann's constant, and T is temperature (in Kelvins). The adjustable parameters of the WLC model are the persistence length (p) and the contour length (L).

The persistence length is a measure of the bending rigidity or stiffness of a polypeptide chain. For a single protein molecule, the persistence length is typically less than 2.0 nm (Carrion-Vazquez et al., 1999; Kellermayer et al., 1997; Müller et al., 1999; Oberhauser et al., 1999; Tskhovrebova et al., 1997), which is similar to the physical length of 0.4 nm between C_α atoms in the backbone of a protein (Mueller et al., 1999). The contour length is the extended length of either an entire protein molecule or a structural domain within a protein. A number of groups have studied the force-structure relationship of ligand-receptor pairs by comparing AFM force spectra to WLC models (Carrion-Vazquez et al., 1999; Lower et al., 2001a, 2005, 2007; Mueller et al., 1999; Oberdorfer et al., 2000; Rief et al., 1997).

For example, if Fn on the tip forms a bond with a receptor on the outer cell wall of a bacterium, an increasingly nonlinear force will be exerted on the tip as the tip is pulled away from the surface of the bacterium (i.e. the separation distance increases

from left to right in a force-distance profile). This process causes the mechanical unfolding of the protein(s) bridging the bacterium to the AFM tip. At some distance from the surface, the force exerted by the tip's spring constant will exceed the tolerance of the ligand/receptor interaction, and the bond will break or the load-bearing domain will unravel. At this point, the tip will "snap" back to its index position, producing a sawtooth-shaped profile or waveform.

Figure 18.6 (solid black curve) shows the WLC force-extension relationship for 525 amino acids ($L = 210$ nm) at the N-terminal domain of Fn. This is the region of Fn that binds to FnBP on *S. aureus* (Foster and Höök, 1998; Greene et al., 1995; Schwarz-Linek et al., 2004). The WLC prediction compares well with the force spectra corresponding to an Fn-coated tip on a glass substrate (Fig. 18.6). There is a nonlinear force-distance (or force-extension) relationship until the Fn breaks free of the glass slide at an extension distance of ~200 nm, which corresponds to the extended length of the N-terminal domains on Fn.

The WLC model can also be used to explain what happens when FnBP on *S. aureus* forms a bond with Fn molecules on the AFM tip. Parallel bonds that form along the length of Fn and FnBP would cause a stiffening (i.e. decreasing persistence length, p, in Eq. (3)) of the protein–protein bond. Figure 18.6 (dotted black curve) shows the hypothetical sawtooth-shaped binding profile for FnBP that forms parallel bonds with the N-terminal region of Fn. For this curve the persistence length was set at 0.04 nm, which is smaller than the physical dimension of an amino acid.

Others have attributed such small values for persistence length to a response caused by multiple protein chains acting in parallel (Bemis et al., 1999; Dugdale et al., 2005, 2006; Higgins et al., 2002; Kellermayer et al., 1997; Lee et al., 2006). For example, ten protein chains in parallel, each with the same contour length, would exert a force ten times that of a single chain. Fitting this response by a single chain model, such as the WLC, would result in one-tenth the true persistence length value. This may be the situation for *S. aureus* FnBP as other studies suggest that one FnBP has the capacity to bind to multiple copies (2–9) of Fn (Fröman et al., 1987; Huff et al., 1994).

18.3.3 Other Uses of AFM: Loading Rate and Affinity Maps

The two examples above provide only small glimpses into the possibilities that AFM offers to investigators who wish to explore the interface between a living bacterium and another surface. Recently, it was demonstrated that individual proteins on the surface of a living bacterium could be mapped across the cell wall (Lower et al., 2009). This was accomplished by tuning into a specific force-signature, like the one shown in Fig. 18.6. Other researchers have begun to use AFM to study the fundamental binding properties (e.g. dissociation rate constant) of protein bonds. These investigations rely upon the fact that the rupture force of a ligand–receptor pair should depend upon the loading rate (N s^{-1}) of the bond (Bell, 1978; Evans, 2001). The loading rate of a bond can be easily manipulated with the AFM by simply

varying the retraction velocity (m s^{-1}) and spring constant (N m^{-1}) of the cantilever. Benoit et al. (2000) and Hanley et al. (2003) provide an excellent description of this work on large eukaryotic cells. This type of research could also be applied to study fundamental aspects of bacterial adhesion.

References

Albrecht TR, Akamine S, Carver TE, Quate CF (1990) Microfabrication of cantilever styli for the atomic force microscope. J Vac Sci Technol A 8:3386–3396

Bell GI (1978) Models for specific adhesion of cells to cells. Science 200:618–627

Bemis JE, Akhremitchev BB, Walker GC (1999) Single polymer chain elongation by atomic force microscopy. Langmuir 15:2799–2805

Benoit M, Gabriel D, Gerisch G, Gaub HE (2000) Discrete interactions in cell adhesion measured by single-molecule force spectroscopy. Nat Cell Biol 2:313–317

Binnig G, Quate CF, Gerber C (1986) Atomic force microscope. Phys Rev Lett 56:930–933

Butt HJ, Kappl M, Mueller H, Raiteri R, Meyer W, Ruhe J (1999) Steric forces measured with the atomic force microscope at various temperatures. Langmuir 15:2559–2565

Camesano TA, Logan BE (2000) Probing bacterial electrosteric interactions using atomic force microscopy. Environ. Sci. Technol. 34:3354–3362

Cappella B, Dietler G (1999) Force-distance curves by atomic force microscopy. Surf Sci Rep 34:1–44

Carrion-Vazquez M, Oberhauser AF, Fowler SB, Marszalek PE, Broedel SE, Clarke J, Fernandez JM (1999) Mechanical and chemical unfolding of a single protein: a comparison. Proc Natl Acad Sci USA 96:3694–3699

Cleveland JP, Manne S, Bocek D, Hansma PK (1993) A nondestructive method for determining the spring constant of cantilevers for scanning force microscopy. Rev Sci Instrum 64:403–405

Craig VSJ, Neto C (2001) *In situ* calibration of colloid probe cantilevers in force microscopy: hydrodynamic drag on a sphere approaching a wall. Langmuir 17:6018–6022

Ducker WA, Senden TJ, Pashley RM (1991) Direct measurement of colloidal forces using an atomic force microscope. Nature 353:239–241

Ducker WA, Senden TJ, Pashley RM (1992) Measurements of forces in liquids using a force microscope. Langmuir 8:1831–1836

Dugdale TM, Dagastine R, Chiovitti A, Mulvaney P, Wetherbee R (2005) Single adhesive nanofibers from a live diatom have the signature fingerprint of modular proteins. Biophys J 89:4252–4260

Dugdale TM, Dagastine R, Chiovitti A, Wetherbee R (2006) Diatom adhesive mucilage contains distinct supramolecular assemblies of a single modular protein. Biophys J 90:2987–2993

Elimelech M, Gregory J, Jia X, Williams R (1995) Particle deposition & aggregation: measurement, modeling, and simulation. Butterworth-Heinemann, Oxford

Evans E (2001) Probing the relation between force – lifetime – and chemistry in single molecular bonds. Annu Rev Biophys Biomol Struct 30:105–128

Flory PJ (1989) Statistical mechanics of chain molecules. Hanser Publisher, Munich, Germany

Foster TJ, Höök M (1998) Surface protein adhesins of *Staphylococcus aureus*. Trends Microbiol 6:484–488

Fröman G, Switalski LM, Speziale P, Höök M (1987) Isolation and characterization of a fibronectin receptor from *Staphylococcus aureus*. J Biol Chem 262:6564–6571

Greene C, McDevitt D, Francois P, Vaudaux PE, Lew DP, Foster TJ (1995) Adhesion properties of mutants of *Staphylococcus aureus* defective in fibronectin-binding proteins and studies on the expression of fnb genes. Mol Microbiol 17:1143–1152

Hanley W, McCarty O, Jadhav S, Tseng Y, Wirtz D, Konstantopoulos K (2003) Single molecule characterization of P-selectin/ligand binding. J Biol Chem 278:10556–10561

Heilmann C, Schweitzer O, Gerke C, Vanittanakom N, Mack D, Götz F (1996) Molecular basis of intercellular adhesion in the biofilm-forming *Staphylococcus epidermidis.* Mol Microbiol 20:1083–1091

Higgins MJ, Crawford SA, Mulvaney P, Wetherbee R (2002) Characterization of the adhesive mucilages secreted by live diatom cells using atomic force microscopy. Protist 153: 25–38

Huff S, Matsuka YV, McGavin MJ, Ingham KC (1994) Interaction of N-Terminal fragments of fibronectin with synthetic and recombinant-D motifs from its binding-protein on *Staphylococcus aureus* studied using fluorescence anisotropy. J Biol Chem 269:15563–15570

Hutter JL, Bechhoefer J (1993) Calibration of atomic-force microscope tips. Rev Sci Instrum 64:1868–1873

Israelachvili JN (1992) Intermolecular and surface forces. Academic, London

Israelachvili JN, McGuiggan PM (1988) Forces between surfaces in liquids. Science 241: 795–800

Jericho SK, Jericho MH, Hubbard T, Kujath M (2004) Micro-electro-mechanical systems microtweezers for the manipulation of bacteria and small particles. Rev Sci Instrum 75: 1280–1282

Kellermayer MSZ, Smith SB, Granzier HL, Bustamante C (1997) Folding-unfolding transitions in single titin molecules characterized with laser tweezers. Science 276:1112–1116

Kendall TA, Lower SK (2004) Forces between minerals and biological surfaces in aqueous solution. Adv Agronom 82:1–54

Klein C, Hurlbut CS (1985) Manual of mineralogy. Wiley, New York, NY

Leckband D, Israelachvili JN (2001) Intermolecular forces in biology. Quart Rev Biophys 34: 105–267

Lee G, Abdi K, Jiang Y, Michaely P, Bennett V, Marszalek PE (2006) Nanospring behaviour of ankyrin repeats. Nature 440:246–249

Lower SK, Hochella MF, Beveridge T (2001a) Bacterial recognition of mineral surfaces: nanoscale interactions between *Shewanella* and alpha-FeOOH. Science 292:1360–1363

Lower BH, Shi L, Yongsunthon R, Droubay TC, McCready DE, Lower SK (2007) Specific bonds between an iron oxide surface and outer membrane cytochromes MtrC and OmcA from S*hewanella oneidensis* MR-1. J Bacteriol 189:4944–4952

Lower SK, Tadanier CJ, Hochella MF (2000) Measuring interfacial and adhesion forces between bacteria and mineral surfaces with biological force microscopy. Geochim Cosmochim Acta 64:3133–3139

Lower SK, Tadanier CJ, Hochella MF (2001b) Dynamics of the mineral-microbe interface: use of biological force microscopy in biogeochemistry and geomicrobiology. Geomicrobiol J 18: 63–76

Lower SK, Tadanier CJ, Hochella MF, Berry DF, Potts M (1999) The bacteria-mineral interface: probing nanoscale forces with biological force microscopy. Geol Soc Am Abstr Prog 31(7):A394

Lower BH, Yongsunthon R, Shi L, Wildling L, Gruber HJ, Wigginton NS, Reardon CL, Pinchuk GE, Droubay TC, Boily JF, Lower SK (2009) Antibody recognition force microscopy shows that outer membrane cytochromes OmcA and MtrC are expressed on the exterior surface of *Shewanella oneidensis* MR-1. Appl Environ Microbiol 75:2931–2935

Lower BH, Yongsunthon R, Vellano FP, Lower SK (2005) Simultaneous force and fluorescence measurements of a protein that forms a bond between a living bacterium and a solid surface. J Bacteriol 187:2127–2137

Mack D, Fischer W, Krokotsch A, Leopold K, Hartmann R, Egge H, Laufs R (1996) The intercellular adhesin involved in biofilm accumulation of *Staphylococcus epidermidis* is a linear beta-1,6-linked glucosaminoglycan: purification and structural analysis. J Bacteriol 178:175–183

Madigan MT, Martinko JM, Parker J (2003) Brock biology of microorganisms. Prentice Hall, Upper Saddle River, NJ

Mueller H, Butt HJ, Bamberg E (1999) Force measurements on myelin basic protein adsorbed to mica and lipid bilayer surfaces done with the atomic force microscope. Biophys J 76: 1072–1079

Müller DJ, Baumeister W, Engel A (1999) Controlled unzipping of a bacterial surface layer with atomic force microscopy. Proc Natl Acad Sci USA 96:13170–13174

Noy A, Vezenov DV, Lieber CM (1997) Chemical force microscopy. Annu Rev Mater Sci 27: 381–421

Oberdörfer Y, Fuchs H, Janshoff A (2000) Conformational analysis of native fibronectin by means of force spectroscopy. Langmuir 16:9955–9958

Oberhauser AF, Marszalek PE, Carrion-Vazquez M, Fernandez JM (1999) Single protein misfolding events captured by atomic force microscopy. Nat Struct Biol 6:1025–1028

Parsek MR, Fuqua C (2004) Biofilms 2003: emerging themes and challenges in studies of surface-associated microbial life. J Bacteriol 186:4427–4440

Prince JL, Dickinson RB (2003) Kinetics and forces of adhesion for a pair of capsular/unencapsulated *Staphylococcus* mutant strains. Langmuir 19:154–159

Razatos A, Ong Y-L, Sharma MM, Georgiou G (1998) Molecular determinants of bacterial adhesion monitored by atomic force microscopy. Proc Natl Acad Sci USA 95:11059–11064

Rief M, Gautel M, Oesterhelt F, Fernandez JM, Gaub HE (1997) Reversible unfolding of individual titin immunoglobulin domains by AFM. Science 276:1109–1112

Schwarz-Linek U, Höök M, Potts JR (2004) The molecular basis of fibronectin-mediated bacterial adherence to host cells. Mol Microbiol 52:631–641

Senden TJ, Ducker WA (1994) Experimental determination of spring constants in atomic-force microscopy. Langmuir 10:1003–1004

Taylor ES, Lower SK (2008) Thickness and surface density of extracellular polymers on Acidithiobacillus ferrooxidans. Appl Environ Microbiol 74:309–311

Tortonese M (1997) Cantilevers and tips for atomic force microscopy. IEEE Eng Med Biol Mag 16:2833

Tskhovrebova L, Trinick J, Sleep JA, Simmons RM (1997) Elasticity and unfolding of single molecules of the giant muscle protein titin. Nature 387:308–312

Watnick P, Kolter R (2000) Biofilm, city of microbes. J Bacteriol 182:2675–2679

Whitman WB, Coleman DC, Wiebe WJ (1998) Prokaryotes: the unseen majority. Proc Natl Acad Sci USA 95:6578–6583

Yongsunthon R, Lower SK (2006) Force measurements between a bacterium and another surface *in situ*. Adv Appl Microbiol 58:97–124

Ziebuhr W, Heilmann C, Götz F, Meyer P, Wilms K, Straube B, Hacker J (1997) Detection of the intercellular adhesion gene cluster (ica) and phase variation in *Staphylococcus epidermidis* blood culture strains and mucosal isolates. Infect Immun 65:890–896